

# Novel Electronic Structures of Ru-Pnictides $RuPn$ ( $Pn = P, As, Sb$ )

H. Goto<sup>1</sup>, T. Toriyama<sup>1</sup>, T. Konishi<sup>2</sup>, and Y. Ohta<sup>1\*</sup>

<sup>1</sup> Department of Physics, Chiba University, Chiba 263-8522, Japan

<sup>2</sup> Graduate School of Advanced Integration Science, Chiba University, Chiba 263-8522, Japan

---

## Abstract

Density-functional-theory-based electronic structure calculations are made to consider the novel electronic states of Ru-pnictides RuP and RuAs where the intriguing phase transitions and superconductivity under doping of Rh have been reported. We find that there appear nearly degenerate flat bands just at the Fermi level in the high-temperature metallic phase of RuP and RuAs; the flat-band states come mainly from the  $4d_{xy}$  orbitals of Ru ions and the Rh doping shifts the Fermi level just above the flat bands. The splitting of the flat bands caused by their electronic instability may then be responsible for the observed phase transition to the nonmagnetic insulating phase at low temperatures. We also find that the band structure calculated for RuSb resembles that of the doped RuP and RuAs, which is consistent with experiment where superconductivity occurs in RuSb without Rh doping.

*Keywords:* Ru-pnictide, electronic structure, metal-insulator transition, superconductivity

---

## 1 Introduction

Physics of transition-metal compounds has long been one of the major themes of strongly correlated electron systems [1]. Recently, superconductivity has been discovered in Ru-pnictides, RuP and RuAs, under Rh doping [2, 3]. These compounds crystallize in a MnP-type orthorhombic structure (space group  $Pnma$ ), in which the  $RuPn_6$  octahedra form a face-sharing chain along the  $a$  axis [4] of the crystal structure (see Fig. 1). The chains are connected by the edges and Ru ions form a distorted triangular lattice in the  $bc$  plane. The one-dimensional zigzag chains of the edge-sharing octahedra  $RuPn_6$  are thus formed along the  $b$  axis of the crystal.

The undoped parent compounds RuP and RuAs show two sequential phase transitions: (i) a weak transition from a metal to a pseudogap phase at 330 K for RuP and at 280 K for RuAs, and (ii) a first-order transition to a nonmagnetic insulator phase at 270 K for RuP and at 200 K for RuAs. By Rh doping, these two phase transitions are suppressed and superconductivity occurs in the vicinity of the pseudogap phase [2, 3].

---

\*ohta@faculty.chiba-u.jp

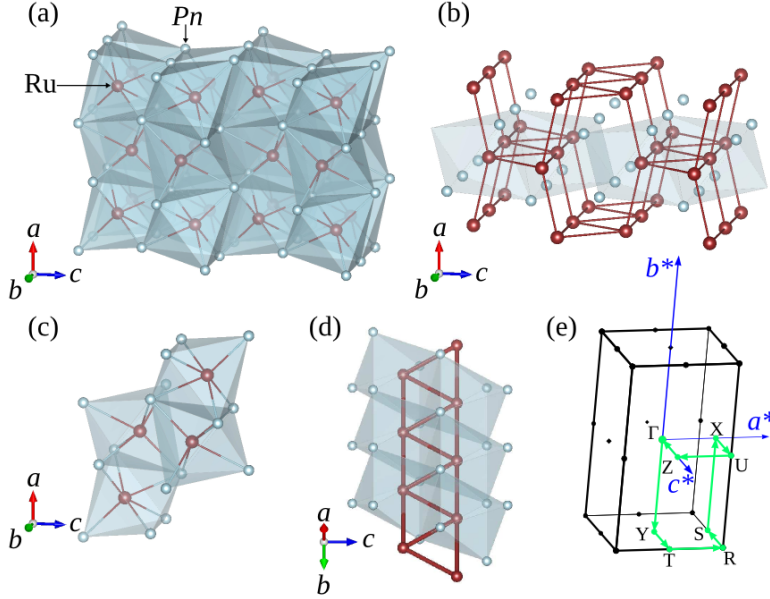


Figure 1: Schematic representations of the crystal structure of  $\text{RuPn}$  ( $Pn = \text{P, As, Sb}$ ), where brown (gray) balls represent the Ru ( $Pn$ ) ions. (a) The three-dimensional arrangement of the  $\text{RuPn}_6$  octahedra, (b) the coupled zigzag chains of Ru ions, (c) the unit cell containing four Ru ions, (d) the zigzag ladder of Ru ions, and (e) the Brillouin zone of  $\text{RuPn}$  in the high-temperature phase.

The Ru  $3d$  core-level and valence-band photoemission spectroscopy experiments on RuP [5] have shown that the Ru valence is +3 with  $t_{2g}^5$  configuration and that the spectral weight near the Fermi level is moderately suppressed in the pseudogap phase, consistent with the pseudogap opening of  $2\Delta/k_B T_c \sim 3$  with the gap size  $\Delta \sim 50$  meV and transition temperature  $T_c \sim 330$  K. It has also been suggested [5] that the electronic orderings responsible for the phase transitions are different from the conventional charge-density-wave ordering because the Ru  $3d$  peak in the photoemission spectrum remains sharp in the pseudogap and insulating phases.

The NMR experiment has also been done for  $\text{Ru}_{1-x}\text{Rh}_x\text{P}$  using  $^{31}\text{P}$  nuclei [6]. It has been shown that, for the undoped RuP, both the Knight shift  $K$  and relaxation rate  $1/T_1 T$  suddenly decrease at 270 K with decreasing temperature, indicating that the density of states at the Fermi level suddenly decreases at 270 K where the transition to the nonmagnetic insulator phase occurs. The temperature dependence of the uniform magnetic susceptibility observed [2] is consistent with this behavior. The energy gap in the nonmagnetic insulating phase at  $x = 0$  is estimated to be 1218 K. The Rh doping suppresses the changes in  $K$  and  $1/T_1 T$  and the antiferromagnetic spin correlation is strongly enhanced in the pseudogap phase at  $x = 0.2$ .

Recently, RuP single crystals were synthesized, whereby the two structural phase transitions have been confirmed. However, it was found that the resistivity drops monotonically upon temperature cooling below the second transition, indicating that the material shows metallic behavior in the lowest temperatures, which is in sharp contrast with the insulating ground state of polycrystalline samples [7]. Optical conductivity measurements were also performed to reveal that a sudden reconstruction of the band structure over a broad energy scale and a significant removal of conducting carriers occur below the first phase transition, while a charge-

density-wave-like energy gap opens below the second phase transition [7]. Thus, there is an essential conflict even in experimental situation; i.e., RuP at low temperatures is insulating in polycrystalline samples but metallic in single-crystalline samples. Possible off-stoichiometry of the single-crystalline samples may be the cause of this discrepancy and further experimental studies are now in progress [8].

In this paper, in order to elucidate the microscopic origins of the two phase transitions and consider the mechanism of superconductivity, we carry out the density-functional-theory (DFT) based electronic structure calculations using WIEN2k [9] and add a number of new aspects to the previous calculation [3]. The basic electronic structures of Ru-pnictides RuP, RuAs, and RuSb, including the effects of Rh doping, are thereby discussed, which will be the first step toward understanding of the novel electronic states of these materials.

We thus find that there appear nearly degenerate flat bands just at the Fermi level in the metallic phase of RuP and RuAs and that these bands come mainly from the  $4d_{xy}$  orbitals of Ru ions. We then suppose that these flat bands indicate an electronic instability, resulting in the structural transition, which may be responsible for the pseudogap formation (or metal-insulator transition) in these systems. Here, possible occurrence of the spin-singlet formation may cause the nonmagnetic insulator phase at low temperatures. The effects of Rh doping on RuP and RuAs are also examined in the virtual crystal approximation and find that the rigid-band approximation works fairly well in these systems. We also calculate the band structure of RuSb and show that this material is significantly different from RuP and RuAs in that its electronic structure without doping resembles that of the doped RuP and RuAs.

## 2 Computational details

We employ the WIEN2k code [9] based on the full-potential linearized augmented-plane-wave method and present the calculated results obtained in the generalized gradient approximation for electron correlations, where we use the exchange-correlation potential of Ref. [10]. The spin-orbit interaction is taken into account as indicated in the calculated results. We use the crystal structures measured at room temperature [4, 11, 12], which have the orthorhombic symmetry (space group  $Pnma$ ) with the lattice constants (in units of Å) of  $a = 5.520$ ,  $b = 3.168$ , and  $c = 6.120$  for RuP,  $a = 5.628$ ,  $b = 3.239$ , and  $c = 6.184$  for RuAs, and  $a = 5.9608$ ,  $b = 3.7023$ , and  $c = 6.5797$  for RuSb. The unit cell contains 4 Ru ions and 4 ligand ions, where all the Ru ions (and ligand ions) are crystallographically equivalent. See Fig. 1 for the sketches of the crystal structure.

In the self-consistent calculations, we use 225, 300, and 270  $\mathbf{k}$ -points in the irreducible part of the Brillouin zone for RuP, RuAs, and RuSb, respectively. We used the muffin-tin radii ( $R_{\text{MT}}$ ) of 2.50 (Ru) and 1.95 (P) for RuP, 2.32 (Ru) and 2.21 (As) for RuAs, and 2.46 (Ru) and 2.46 (Sb) for RuSb in units of Bohr, and assume the plane-wave cutoff of  $K_{\text{max}} = 7.00/R_{\text{MT}}$ . We use the codes VESTA [13] and XCrySDen [14] for graphical purposes.

## 3 Results and discussion

### 3.1 Densities of states

First, let us discuss the densities of states (DOS) of  $\text{RuP}n$ , which are shown in Fig. 2. We find that the topmost core  $s$ -orbital states of the ligand ions are located around  $-12$  eV. We then find that the  $4d$  orbitals of Ru ions contribute to the DOS in a wide energy region between

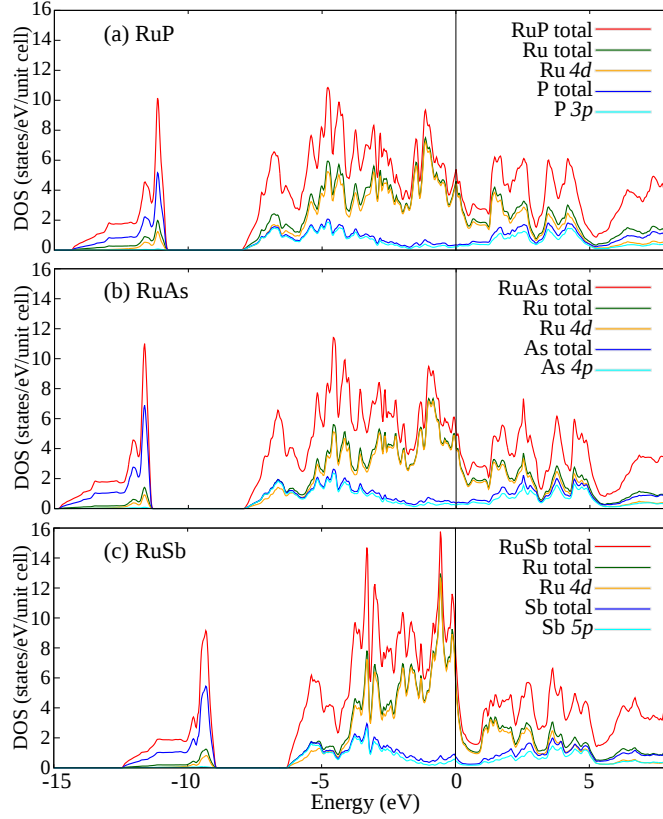


Figure 2: Calculated densities of states (DOS) of (a) RuP, (b) RuAs, and (c) RuSb. The Fermi level is set to be the origin of energy and is indicated by the vertical line. The spin-orbit interaction is taken into account only for RuSb.

−8 eV and 5 eV and the states near the Fermi level are mainly come from the  $4d t_{2g}$  orbitals of Ru ions. The states coming from the  $3p$  ( $4p$ ) orbitals of P (As) ions are also extended in a wide energy range between −8 eV and 5 eV, which are thus largely overlapped with the  $4d$  states of Ru ions. More precisely, the states of the  $3p$  ( $4p$ ) orbitals of P (As) ions are mainly located in the lower (between −8 and −2 eV) and higher (between 1.5 and 5 eV) energy regions and thus their contribution is rather small near the Fermi level. These results are in agreement with results of the previous calculation [3]. A sharp peak-like structure appears just at the Fermi level of the DOS of RuP and RuAs, which comes from the flat bands discussed in the next subsection. The situation of RuSb is rather different from that of RuP and RuAs as seen in Fig. 2(c). This occurs because the  $5p$  states of Sb are located rather high in energy than those of the  $3p$  ( $4p$ ) states of P (As), as will be seen in Fig. 3. Also noted is that the overall band width is rather narrower in RuSb than in RuP and RuAs, which is because the lattice constants of RuSb are considerably larger than those of RuP and RuAs, leading to a smaller hybridization and thus to the narrower band width in RuSb. The values of the DOS at the Fermi level are 5.33 for RuP, 5.09 for RuAs, and 8.12 for RuSb in units of states/eV/unit cell.

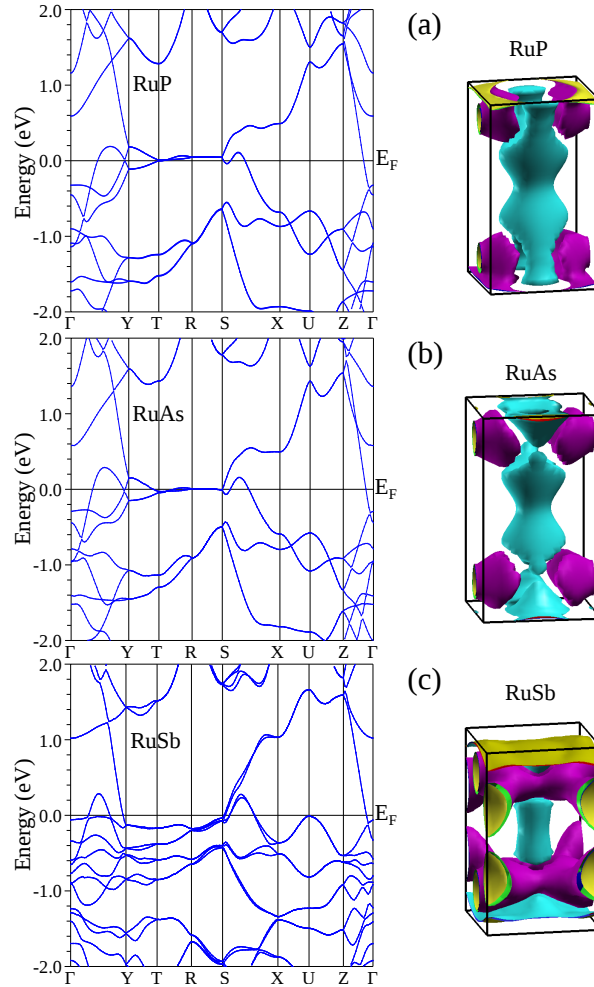


Figure 3: Calculated band dispersions and Fermi surfaces of (a) RuP, (b) RuAs, and (c) RuSb. The Fermi level is indicated by the horizontal line. The spin-orbit interaction is taken into account only for RuSb.

### 3.2 Band dispersions and Fermi surfaces

The calculated band dispersions and Fermi surfaces are shown in Fig. 3. There are 32 bands in the energy range between  $-8$  eV and  $+5$  eV, 8 of which are from the  $e_g$  orbitals of 4 Ru ions in the unit cell and other 24 of which are from the  $t_{2g}$  orbitals of 4 Ru ions and  $p$  orbitals of the 4 ligand ions. There are 44 valence electrons in the unit cell, such that the top 8 bands coming mainly from the  $e_g$  orbitals of Ru are above the Fermi level, the next 4 bands coming mainly from the  $t_{2g}$  orbitals of Ru cross the Fermi level, and the lower 20 bands coming from the  $t_{2g}$  of Ru and  $p$  orbitals of ligand ions are below the Fermi level.

Near the Fermi level, we find four (or two doubly degenerate) bands consisting mainly from the  $4d_{xy}$  orbitals of Ru, which form very flat bands just at the Fermi level in RuP and RuAs, in

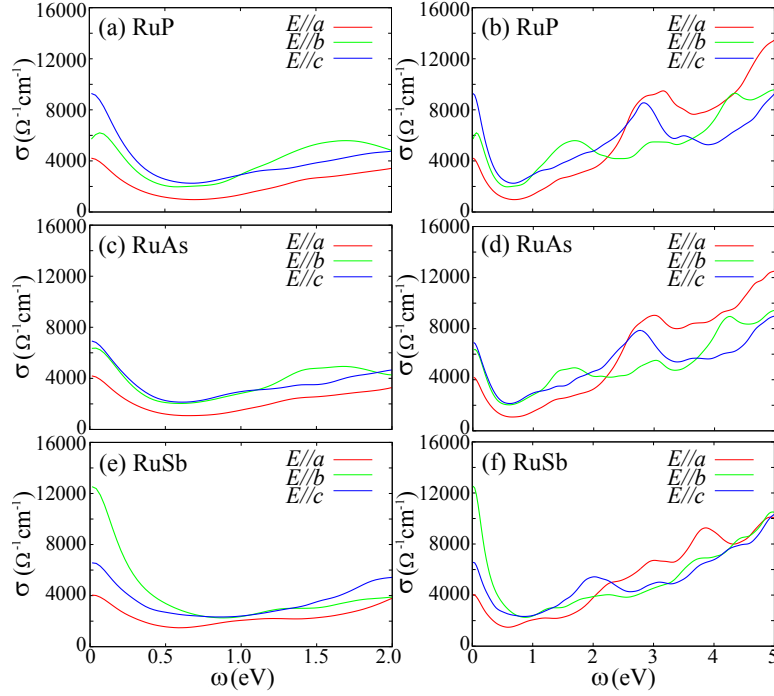


Figure 4: Calculated optical conductivity spectra  $\sigma(\omega)$  of RuP [(a) and (b)], RuAs [(c) and (d)], and RuSb [(e) and (f)], where  $E$  is the applied electric field. The spin-orbit interaction is taken into account. Low-energy (high-energy) regions of the spectra are shown in the left (right) panels.

agreement with a previous calculation [3]. The flat-band states are located around the Y, T, R, and S points (or at the edge  $k_y = \pm\pi/b$ ) of the Brillouin zone [see Fig. 1(e) for the definition]. The two bands of the four are mainly above the Fermi level and the other two band are mainly below the Fermi level, so that the semimetal-like Fermi surfaces of an equal number of electrons and holes are formed as shown in Fig. 3. In RuSb, the situation is somewhat different; i.e., there are the flat bands (though rather deformed) but they are slightly below the Fermi level by  $\sim 0.2$  eV, indicating that a small number of electrons is transferred from the ligand ions. Thus, the Fermi surfaces of RuP and RuAs have the similar topology, which are however very different from the Fermi surface of RuSb. No clear nesting features are observed in the calculated Fermi surfaces of the present materials.

The effects of Rh doping for Ru are also examined by the virtual crystal approximation. We find that the doping shifts the Fermi level upward without any significant changes in the band structure; i.e., the rigid band approximation works well. Thus, the effect of doping of Rh in RuP and RuAs results in the situation similar to the band structure of RuSb. This result is consistent with the experimental fact that the superconductivity occurs by doping of Rh in RuP and RuAs, which occurs without Rh doping in RuSb [2].

We also suggest that the degenerate flat bands at the Fermi level in RuP and RuAs should cause the electronic instability in these systems, the splitting of which may explain the insulating or pseudogap situation observed in these materials. Further experimental and theoretical studies are required for clarifying the situations.

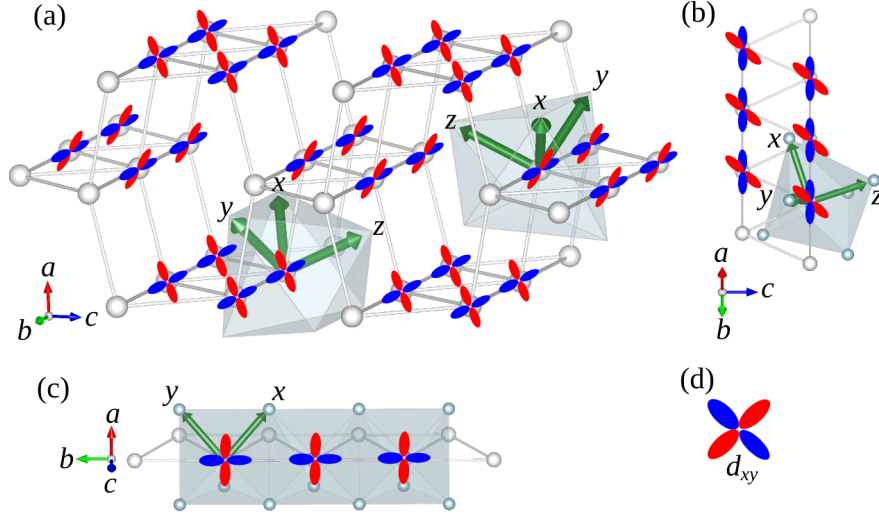


Figure 5: Arrangement of the  $4d_{xy}$  orbitals of Ru ions in  $RuPn$  forming the electronic states near the Fermi level.

### 3.3 Optical conductivity

We calculate the real part of the optical conductivity tensor  $\Re\sigma_{\alpha\beta}(\omega)$  in the random-phase approximation using the results of our electronic structure calculations [15]. The results are shown in Fig. 4, where both the interband and intraband (or Drude) contributions are included. For the Drude contributions, we assume the form

$$\Re\sigma_{\alpha\beta}(\omega) = \frac{\omega_{p,\alpha\beta}^2}{4\pi} \frac{\Gamma}{\omega^2 + \Gamma^2}, \quad (1)$$

where  $\omega_{p,\alpha\beta}$  is the plasma frequency calculated from the band structure and  $\Gamma$  is a lifetime broadening ( $\Gamma = 0.10$  and  $0.30$  eV are assumed for the spectra of  $E \parallel a, b$  and  $E \parallel c$ , respectively). The calculated values of the plasma frequency are 2.502, 2.858, and 3.709 eV for the electric field along the  $a$ ,  $b$ , and  $c$  axes, respectively, for RuP; 2.496, 3.056, and 3.204 eV for RuAs; and 2.445, 4.305, and 3.113 eV for RuSb. The results for RuP can be compared with recent experimental data observed for a single-crystalline RuP [7]. We find that there is a double-peak structure in the calculated spectrum of  $E \parallel b$  in a wide energy range up to  $\sim 4$  eV, which is in fair agreement with experiment. A low-energy dip-like structure at  $\sim 0.5$  eV just above the Drude peak is also consistent with experiment. The temperature variation of the spectra should be studied further to clarify the mechanism of the observed phase transitions.

### 3.4 States near the Fermi level

To analyze the states near the Fermi level further, we calculate the orbital components of the states using the weight plots of the band dispersions and orbital-decomposed partial densities of states (although the detailed results are not shown here). We then find that the flat-band states at the Fermi level in RuP and RuAs are constructed mainly by the  $4d_{xy}$  orbitals of Ru ions, which are illustrated schematically in Fig. 4; i.e., the relevant  $4d_{xy}$  orbitals are located on the one-dimensional zigzag ladder of Ru ions running along the  $b$  direction of the crystal

axis. The zigzag ladders are then connected in the  $ab$  plane to form the three-dimensional crystal structure. Thus, the low-energy effective model of the present material may be given by the connected zigzag ladders of the  $4d_{xy}$  orbitals. We anticipate that the structural instability in RuP and RuAs may well reside in this effective model; for further analysis, experimental determination of the low-temperature crystal structures of RuP and RuAs is highly desirable.

Also noted is that, if we assume the ionization state of  $\text{Ru}^{3+}$ , as was observed in the x-ray photoemission spectroscopy experiment [5], then the filling of 5 electrons in the  $4d$  ( $t_{2g}$ ) orbitals of a Ru ion, so that the ligand ions are in the ionization state of  $3-$  having  $p^6$  electrons. The location of the  $p$  orbitals of the ligand ions are important in the present systems because the  $p$  orbitals are overlapped largely with the  $4d$  orbitals of Ru ions and thus the electrons can flow from the ligand ions to the  $4d$  orbitals of Ru, resulting in the shift of the Fermi level. This is in particular the case when we consider the results for RuSb.

Further analyses of the effective model will be presented in future publications.

## 4 Summary

Motivated by the recent discovery of the nonmagnetic insulating and pseudogap phases, together with superconductivity under Rh doping, in Ru-pnictides RuP, RuAs, and RuSb, we have carried out the DFT-based electronic structure calculations for these materials and have clarified their basic electronic structures responsible for the observed novel electronic properties. We have shown the following: (i) The  $4d$ -orbital states of Ru are hybridized strongly with the  $p$ -orbital states of the ligand ions in the entire energy range between  $-8$  and  $5$  eV around the Fermi level. (ii) The states near the Fermi level are constructed mainly by the  $4d_{xy}$  orbitals of Ru ions, which form the one-dimensional zigzag ladders connected in the MnP-type crystal lattice. (iii) There appear the fourfold nearly degenerate flat bands just at the Fermi level in RuP and RuAs, which are located  $\sim 0.2$  eV below the Fermi level in RuSb. The flat bands come mainly from the  $4d_{xy}$  orbitals of Ru ions. (iv) The doping of Rh ions in RuP and RuAs shifts the Fermi level just above the flat bands in a rigid-band-like manner, producing the similar electronic state near the Fermi level obtained for the undoped RuSb. (v) The calculated optical conductivity spectra of RuP are in fair agreement with experiment in the wide energy range.

We hope that further experimental and theoretical studies will be done in future for clarifying the origins of the observed intriguing properties of these materials and elucidating the mechanism of superconductivity.

## 5 Acknowledgments

We thank D. Hirai, M. Itoh, Y. Kobayashi, S. Li, and T. Mizokawa for providing us with useful information and discussions on Ru-pnictides. This work was supported in part by Futaba Electronics Memorial Foundation and by a Grant-in-Aid for Scientific Research (No. 26400349) from JSPS of Japan. T.T. acknowledges support from the JSPS Research Fellowship for Young Scientists.

## References

- [1] D. I. Khomskii, *Transition Metal Compounds* (Cambridge University Press, 2014).
- [2] D. Hirai, T. Takayama, D. Hashizume, and H. Takagi, Phys. Rev. B **85**, 140509(R) (2012).
- [3] D. Hirai, PhD thesis (Univ. Tokyo, 2011).

- [4] S. Rundqvist, *Acta Chem. Scand.* **16**, 287 (1962).
- [5] K. Sato, D. Ootsuki, Y. Wakisaka, N. L. Saini, T. Mizokawa, M. Arita, H. Anzai, H. Namatame, M. Taniguchi, D. Hirai, and H. Takagi, arXiv:1205.2669.
- [6] S. Li, Y. Kobayashi, M. Itoh, D. Hirai, and H. Takagi, presented at Japanese Physical Society Autumn Meeting (2014).
- [7] R. Y. Chen, Y. G. Shi, P. Zheng, L. Wang, T. Dong, and N. L. Wang, *Phys. Rev. B* **91**, 125101 (2015).
- [8] D. Hirai, private communication.
- [9] P. Blaha, K. Schwarz, G. K. H. Madsen, D. Kvasnicka, and J. Luitz, *WIEN2k* (Technische Universität Wien, Austria, 2002).
- [10] J. P. Perdew, K. Burke, and M. Ernzerhof, *Phys. Rev. Lett.* **77**, 3865 (1996).
- [11] R. D. Heyding and L. D. Calvert, *Can. J. Chem.* **39**, 955 (1961).
- [12] K. Endresen, S. Furuseth, K. Selte, A. Kjekshu, T. Rakke, and A. F. Andresen, *Acta Chem. Scand. A* **31**, 249 (1977).
- [13] K. Momma and F. Izumi, *J. Appl. Crystallogr.* **44**, 1272 (2011).
- [14] A. Kokalj, *Comp. Mater. Sci.* **28**, 155 (2003).
- [15] C. Ambrosch-Draxl and J. O. Sofo, *Comput. Phys. Commun.* **175**, 1 (2006).